BMC Musculoskeletal Disorders

RESEARCH

Open Access

Comprehensive bioinformatics analysis uncover molecular pathways shared between osteoarthritis and atherosclerosis

Yingchao Jin[1] and Hua Zhang[1*]

Abstract

Background There is growing evidence of an association between osteoarthritis (OA) and atherosclerosis (AS). However, their mechanisms are not yet fully understood. The aim of this study was to investigate the common genetic and molecular mechanisms underlying the common pathogenesis of OA and AS.

Methodology Gene expression profiles of OA (GSE51588) and AS (GSE100927) were obtained from the Gene Expression Omnibus (GEO) database. After identifying shared differentially expressed genes (DEGs) and hub genes, we performed multifaceted bioinformatics analyses, including functional annotation, co-expression analysis, TF-mRNA and ceRNA regulatory network construction, pharmacogenetic prediction, and receiver operator characteristic (ROC) curve assessment. In addition, the immune infiltration of OA and AS was analyzed and compared based on the ssGSEA algorithm, and the correlation between hub genes and infiltrating immune cells was evaluated in OA and AS, respectively.

Result A total of 48 up-regulated and 43 down-regulated public DEGs were screened between GSE51588 and GSE100927, and functional enrichment analysis emphasized the important role of immune and inflammatory pathways in OA and AS. After protein-protein interaction (PPI) network construction, a total of 9 hub genes (*CCR5*, *IFIT2*, *MMP1*, *CXCL9*, *RSAD2*, *IFIH1*, *TNF*, *IFIT3*, and *TBX21*) were identified as key genes. Targeting the key genes we identified several molecular drug candidates against OA combined with AS related. Additionally diagnostic efficacy assessment using 9 central genes showed great diagnostic value (area under the curve from 0.710 to 0.973). Immune infiltration study also revealed coordinated changes in immune cell profiles in OA and AS diseases.

Conclusion After a series of bioinformatics analysis and validation, *CCR5*, *IFIT2*, *MMP1*, *CXCL9*, *RSAD2*, *IFIH1*, *TNF*, *IFIT3* and *TBX21* were identified as common hub genes for the development of OA and AS. This study provides a new perspective on the common molecular mechanisms between OA and AS, and offers new insights into the potential pathogenesis of OA combined with AS and the direction of treatment.

Keywords Osteoarthritis, Atherosclerosis, Bioinformatics, Molecular mechanisms, Inflammation, Immunity

*Correspondence:
Hua Zhang
13785067094@163.com
[1]Department of orthopaedics, The Second Hospital of Hebei Medical University, Shijiazhuang, China

© The Author(s) 2025. **Open Access** This article is licensed under a Creative Commons Attribution-NonCommercial-NoDerivatives 4.0 International License, which permits any non-commercial use, sharing, distribution and reproduction in any medium or format, as long as you give appropriate credit to the original author(s) and the source, provide a link to the Creative Commons licence, and indicate if you modified the licensed material. You do not have permission under this licence to share adapted material derived from this article or parts of it. The images or other third party material in this article are included in the article's Creative Commons licence, unless indicated otherwise in a credit line to the material. If material is not included in the article's Creative Commons licence and your intended use is not permitted by statutory regulation or exceeds the permitted use, you will need to obtain permission directly from the copyright holder. To view a copy of this licence, visit http://creativecommons.org/licenses/by-nc-nd/4.0/.

Introduction

Osteoarthritis (OA) is a highly prevalent, age-related joint disease, especially among older adults with multiple comorbidities [1]. Osteoarthritis, as a degenerative joint disease, is characterized by a variety of symptoms, including joint pain, swelling, stiffness, and limited range of motion [2, 3]. OA can seriously affect patients' daily activities and quality of life [4]. According to statistics, OA affects approximately 3.3% of the global population [5]. This imposes a huge health burden on individuals, societies and governments [6, 7]. Atherosclerosis (AS) is a chronic vascular disease characterized by a pathology of fatty deposits in the vessel wall leading to an inflammatory and proliferative cascade [8]. Cardiovascular disease is the leading cause of death worldwide, and the underlying cause of cardiovascular disease is atherosclerosis [9]. Despite its epidemiologic importance, the underlying mechanisms of AO and AS remain poorly understood, and there is an urgent need to investigate the molecular pathways leading to their development and to identify diagnostic and prognostic biomarkers.

There is growing evidence that vascular pathology plays a role in the pathogenesis of knee osteoarthritis [10, 11]. Patients with osteoarthritis commonly also have AS. The relationship between the two diseases were previoisly investigated, and some connections are obvious. Without vascular interactions, bone tissue would not form [12, 13]. Moreover, vascular system diseases may affect to bone metabolism. Some scholars had proposed the concept of bone-vascular axis [14, 15], encompassing a bidirectional flow of cellular, endocrine, and metabolic signals between the vasculature and the skeleton. It is also posed that the disruption of the bone-vascular axis lead to both vascular and skeletal disorders [15]. They suggested that there is a bidirectional flow of cellular, endocrine, and metabolic signals between the vasculature and the skeleton, and that when metabolic dysregulation causes disruption of the bone-vascular axis, the human body may experience both vascular and skeletal disorders [15]. In OA, the pathologic features of inflammatory synovitis, subchondral osteosclerosis and articular cartilage degeneration are augmented with the presence of abnormal vascular line-breaking markings within the subchondral bone [16].H-type EC (which can release MMP and other proteases) can help digest cartilage templates during longitudinal bone growth, which may promote cartilage degeneration in OA [17].It has been shown that while angiogenesis can be inhibited by inhibiting *MMP* and TGFβ signaling, this approach also reduces the abundance of H-type EC and attenuates articular cartilage degeneration [16].In addition, hypervascularization leads to inflammatory cell infiltration and upregulation of local nociceptive receptor expression, resulting in structural damage and nociceptive transmission [18].Inflammatory cell infiltration in OA may be driven by elevated levels of pro-angiogenic factors (including a variety of cytokines, growth factors, and chemokine receptors), which erode subchondral and articular cartilage and thus contribute to the progression of OA [19].

Recent development of bioinformatic techniques has enabled us to gain a deeper understanding of disease pathogenesis at the gene expression level [20]. Common transcriptional features may provide new perspectives on the common pathogenesis of OA and AS. There have been many articles analyzing OA or AS datasets from a single disease perspective, mining potential targets and regulatory biological pathways for OA or AS, respectively [4, 6, 8, 9]. These studies have provided a lot of insights and research directions into the pathogenesis of single diseases of OA or AS, but there has never been a comprehensive study exploring the commonalities of the two diseases of OA and AS. The common transcriptional and regulatory features of the two diseases may provide new ideas for common pathogenesis and therapeutic options for OA and AS.In view of this, the aim of our study was to explore the pathogenesis of OA combined with AS and to explore potential biomarkers and therapeutic directions for both diseases. Our study may provide new clues to investigate the common pathogenesis of OA and AS and to develop relevant diagnostic and treatment programs.

Materials and methods

Dataset preparation

Datasets GSE51588 and GSE100927 were downloaded from the Gene Expression Omnibus (GEO,http://www.ncbi.nlm.nih.gov/geo/) database. The GSE51588 dataset contains 40 subchondral bone samples from patients with OA and 10 subchondral bone samples from healthy humans as a control group. The GSE100927 dataset consists of 69 peripheral artery samples from patients with atherosclerotic lesions and 35 peripheral arterial samples from a healthy population.

Identify DEGs and DEGs shared between OA and AS

We used the "limma" package of R software (version 4.1.1) to perform differential analysis to identify DEGs between OA and non-OA. Our criteria for screening differentially expressed genes were set as adj. P. Val < 0.05 and |log fold change (FC)|>0.585, i.e., a fold difference of 1.5. We then used the Pheatmap, EnhancedVolcano and ggplot2 packages of the R software (version 4.1.1) to convert the results of the variance analysis into heatmaps and volcano maps for presentation. The screening of DEGs between AS and non-AS and the standard setting were the same as in the previous method. Finally, we defined the genes that were simultaneously up-regulated or simultaneously down-regulated in GSE51588 and GSE100927 as overlapping DEGs and used the

"VennDiagram" package of the R software to draw the Wayne diagrams of overlapping DEGs.

Enrichment analysis of overlapping DEGs

Overlapping DEGs were analyzed for Gene Ontology (GO) (including (biological processes, cellular components and molecular functions)) and Kyoto Encyclopedia of Genes and Genomes (KEGG) pathways, respectively. The filter condition for enrichment analysis was defined as p-value < 0.05, which was satisfied to make the enrichment result significant. The 'org.Hs.eg.db' package of the R software was used for gene ID conversion, the 'clusterProfiler' package was used for enrichment analysis to produce results, and packages such as the 'enrichplot' package, the 'RColor' package, and the 'ggplot2' package were used to visualize the results of the enrichment analyses obtained.

Construction of PPI network

The Search Tool for the Retrieval of Interacting Genes (STRING;http://string-db.org) (version 12.0) can be used to search for relationships between proteins, such as direct binding relationships, or co-existing upstream and downstream regulatory relationships, etc., and analyze them in a complex way to produce a PPI network diagrams with complex regulatory relationships. We set interactions with a composite score of more than 0.4 to be statistically significant and hid stray nodes. Cytoscape (http://www.cytoscape.org) (version 3.9.1) can be used to process the resulting PPI network graphs. The Cytoscape software is used to adjust the PPI network graphs and to visualize the PPI network. Cytoscape software was used to adjust the PPI network map and visualize the PPI network. We then applied the Molecular Complex Detection (MCODE) plug-in of Cytoscape to analyze the key functional modules, we set the selection criteria to Degree Cutoff = 2, Node Score Cutoff = 0.2, K-Core = 2 and Max Depth = 100, and plotted the results of the resulting analysis into sub-networks. network.

Identification and analysis of hub genes

CytoHubba is a commonly used plug-in for Cytoscape software, which can be used to simulate and calculate the core protein genes of known PPI networks [21]. There are 12 algorithms in CytoHubba, all of which have been shown to be effective in screening Hub genes. To improve accuracy, we selected four commonly used algorithms from the CytoHubba plugin, including two local-based algorithms (Degree and MCC) and two global-based algorithms (Closeness and EPC), to compute the top 15 core genes. We identified the intersecting genes obtained from the results of the above four algorithm runs as key genes and visualized the results using the "VennDiagram" package of the R software. The GeneMANIA (https://genemania.org) website, a reliable tool for identifying associations within gene sets, can be used to construct co-expression networks of identified core genes. Given a list of queries, the GeneMANIA database can be used to identify an extended list of similar genes using genomics and proteomics data identification functions.

Enrichment analysis of hub genes

The core DEGs were analyzed again for Gene Ontology (GO) (including (biological processes, cellular components and molecular functions)) and Kyoto Encyclopedia of Genes and Genomes (KEGG) pathways, respectively. The filter condition for enrichment analysis was defined as a p-value < 0.05, which was satisfied to make the enrichment result significant. The 'org.Hs.eg.db' package of the R software was used for gene ID conversion, the 'clusterProfiler' package was used for enrichment analysis to produce results, and packages such as the 'enrichplot' package, the 'RColor' package, and the 'ggplot2' package were used to visualize the results of the enrichment analyses obtained.

Construction of a multi-factor regulatory network

The multi factor regulatory network we constructed is divided into two steps. The first step is to use the Sentence Based Text Mining (TRRUST) database(https://www.grnpedia.org/trrust/)To predict the TF of hub genes. After prediction, a regulatory network of TF mRNA was constructed and visualized using Cytoscape software. In the second step, to further investigate the regulatory mechanisms of the corresponding core genes in the TF mRNA network, we used three databases to predict the miRNA targets of Hub genes, including miRanda, miRDB, and Targeted Scan. In addition, the interaction mode between lncRNA and miRNA was predicted by the shotgunScan database. Cytoscape is used to construct ceRNA networks between lncRNA, mRNA, and miRNA.

OA and AS co-potential drug selection

Screening drug molecules based on gene targets is an effective new approach to the molecular study of disease drugs, which can help drug developers to expand the scope of research on relevant drugs and shorten the process of drug development. In this study, we screened relevant drugs targeting the Hub gene through the Drug Signatures Database (DSigDB) (https://dgidb.genome.wustl.edu/), and the results were presented as network diagr ams using Cytoscape software.

Diagnostic performance analysis of hub genes

Diagnostic performance of Hub genes was evaluated using standardized OA and AS gene expression matrix files (GSE51588 and GSE100927). The Hub genes were analyzed and identified using the "reshape2" and

"ggpubr" packages in R. The expression data were converted into ggplot2 input files for plotting box plots. We assessed the diagnostic performance of the resulting core genes by plotting receiver operator characteristic (ROC) curves and observing the area under the curve (AUC). ROC curve analysis was performed using the "pROC" package of the R software and the results were visualized using the "ggplot2" package.

Immune infiltration analysis

ssGSEA (Single Sample Gene Set Enrichment Analysis) is a ranking-based algorithm, a modification of the standard gene set enrichment analysis, which calculates scores representing the absolute enrichment of specific gene sets in each sample [22, 23]. The ssGSEA score was used to quantify the infiltration of immune cells in OA or AS tissue and to determine the level of immune infiltration for each sample in the dataset. Principal component analysis (PCA) was performed to analyze the 28 immune cell infiltration matrix data and find differences between groups. We then used the ggplot2 package to plot violin maps. Spearman correlation analysis was used to determine the correlation between 9 hub genes and 28 immune cells to reveal the relationship between hub genes and immune cells, and the correlation heatmap was constructed using the R language software ggplot2 package.

Statistical analysis

We applied the statistical software R version 4.3.0 for statistical analysis, setting a p value < 0.05 to indicate statistical significance. In all legends of this study, data are expressed as mean ± SEM: $^{*}p < 0.05$, ** $p < 0.01$, *** $p < 0.001$.

Results

Identification of DEGs for OA and AS

A total of 1561 differentially expressed genes were screened from the OA combined dataset (GSE51588) with a p-value < 0.05 and $|\log2FC| > 0.58$ as the screening criteria. Figure 1A and C show the DEG distribution between OA patients and normal controls by heatmaps and volcano plots, respectively. Similarly, a total of 1654 differentially expressed genes were screened from the AS combined dataset (GSE100927) with the same screening criteria of p-value < 0.05 and $|\log2FC| > 0.58$. Figure 1B and D show the distribution of DEGs between AS patients and normal controls by heatmaps and volcano plots, respectively. By Venn diagram (Fig. 1E and F), we identified 91 overlapping DEGs between GSE51588 and GSE100927, including 48 overlapping high-expression DEGs and 43 overlapping low-expression DEGs.

Enrichment analysis of overlapping DEGs

In order to analyze the biological functions and pathways involved in these overlapping genes, we performed GO and KEGG enrichment analysis using the "clusterProfiler" package of R software. GO (Fig. 2A, B) analysis showed that these overlapping genes were predominantly enriched in the following terms: Biological processes (BP) include extracellular matrix organization, extracellular structure organization, external encapsulating structure organization, response to virus, defense response to virus, defense response to symbiont and response to copper ion, etc., Cell components (CC) include collagen – containing extracellular matrix, collagen trimer, complex of collagen trimers, high – density lipoprotein particle, plasma lipoprotein particle, lipoprotein particle and protein – lipid complex, etc.; Molecular functions (MF) include endopeptidase activity, endopeptidase activity, serine – type peptidase activity, serine hydrolase activity, Endopeptidase activity, and Endopeptidase activity. extracellular matrix structural constituent, extracellular matrix structural constituent conferring tensile strength and metalloendopeptidase activity.In the enrichment analysis of KEGG (Fig. 2C, D) pathway, overlapping genes were mainly related to the following pathways. Including Mineral absorption, Cytokine – cytokine receptor interaction, Salmonella infection, Inflammatory bowel disease, Viral protein interaction with cytokine and cytokine receptor, Protein digestion and absorption, NF – kappa B signaling pathway and Apoptosis, etc. The results suggest that the common differential genes shared by OA and AS are associated with inflammatory and immune responses and are highly relevant to their pathogenesis.

Construction and module analysis of PPI network

The network of relationships between proteins can be searched on the STRING database based on overlapping genes (Fig. 3A), based on which we constructed a PPI network of overlapping DEGs using the Cytoscape software provided that the composite score was > 0.4. This network consists of 59 nodes and 168 edges (Fig. 3B). Five tightly linked gene modules, including 29 common DEGs and 67 interaction pairs, were obtained through the MCODE plug-in of Cytoscape software (Fig. 4A-E).

Selection and analysis of key genes

We installed the cytoHubba plugin within the Cytoscape software. With the four algorithms commonly used by the cytoHubba plugin, including two local-based algorithms (Degree and MCC) and two global-based algorithms (Closeness and EPC), we calculated the top 15 ranked key genes (Fig. 5A-D). After intersecting the key genes obtained from the four algorithms using a Venn diagram, we obtained nine common hub genes, including

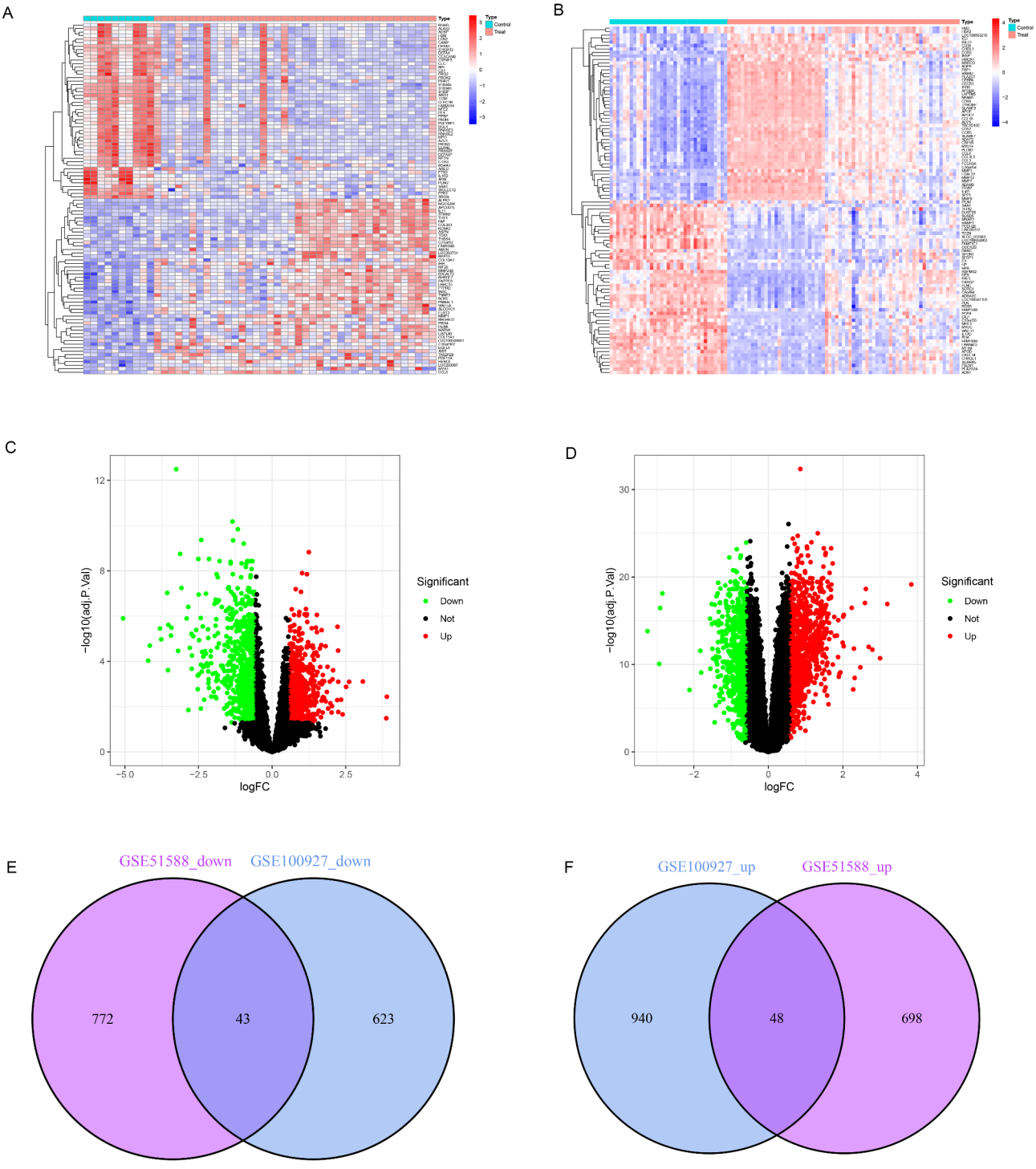

Fig. 1 DEGs in datasets GSE51588 and GSE100927. **a**: heatmap of GSE51588. **b**: heatmap of GSE100927. **c**: volcano map of GSE51588. **d**: volcano map of GSE100927. **e**: 43 overlapping low-expression DEGs shared by GSE51588 and GSE100927. **f**: 48 overlapping highly expressed DEGs shared by GSE51588 and GSE100927. DEG, differentially expressed gene

CCR5, *IFIT2*, *MMP1*, *CXCL9*, *RSAD2*, *IFIH1*, *TNF*, *IFIT3*, and *TBX21* (Fig. 5E).

Based on the GeneMANIA database, we produced a gene interaction network to analyze the related functions of these key genes (Fig. 6). These genes showed a complex PPI network with 60.75% co-expression, 31.17% physical interaction, 7.51% prediction and 0.56% co-localization. The results also showed that they are mainly associated with response to viruses and cellular response to interferons. These key genes could not only

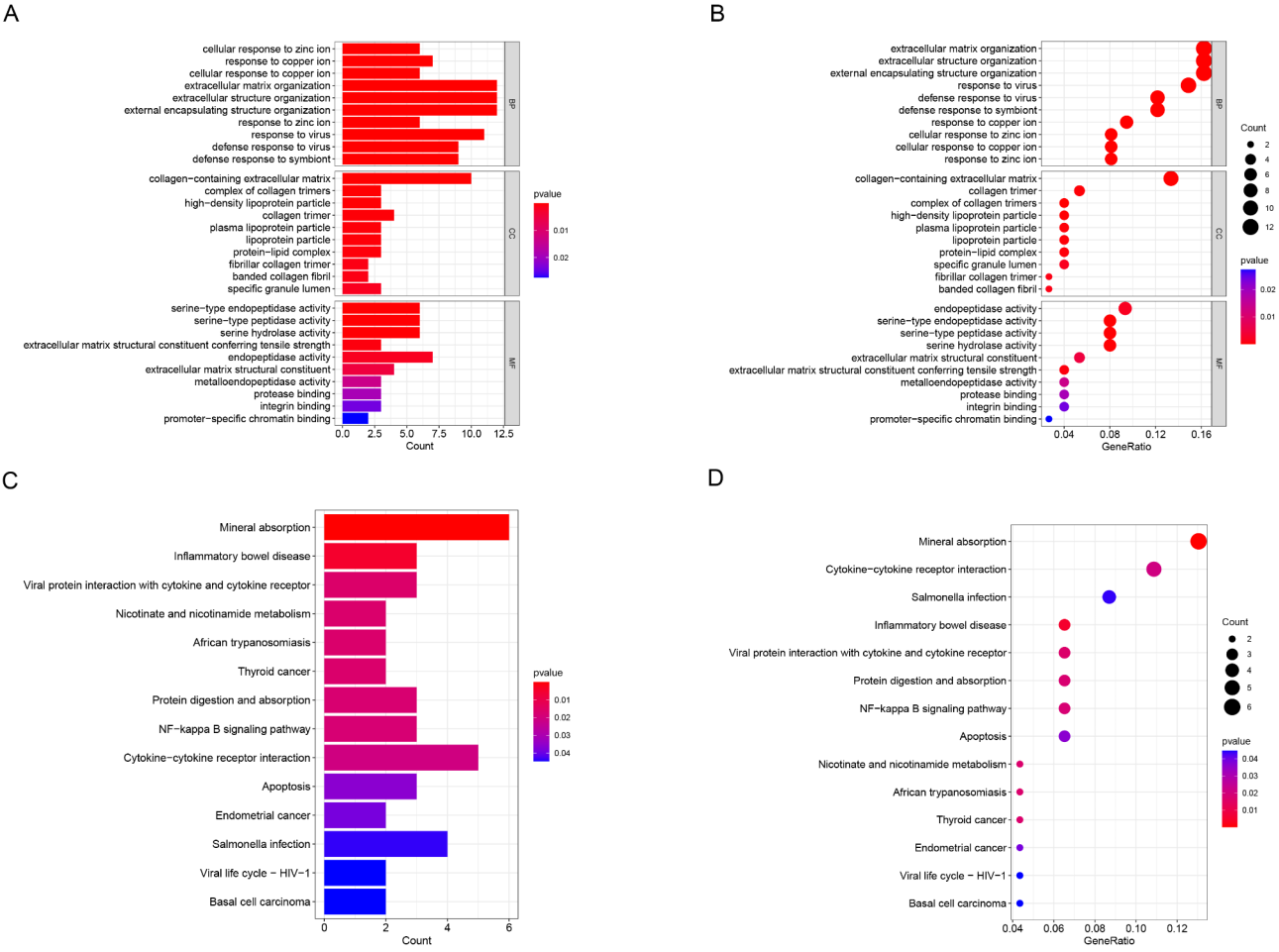

Fig. 2 Functional enrichment analysis of common DEGs. **a**, **b**: Functional enrichment clustering analysis of common DEGs using GO terms in biological processes, cellular components and molecular functions. (**A** is shown as a bar chart. **B** is shown as a bubble chart); **C**, **D**: KEGG pathway analysis of common DEGs. (**C** is shown as a bar chart. **D** is shown as a bubble chart.) GO: gene ontology; KEGG: Kyoto Encyclopedia of Genes and Genomes

be potential biomarkers, but may also provide new therapeutic options for the studied diseases.

Enrichment analysis of hub genes

In order to analyze the biological functions and pathways involved in the resulting Hub genes, we again performed GO and KEGG enrichment analysis using the "clusterProfiler" package of R software. GO (Fig. 7A) analysis showed that these overlapping genes were mainly enriched in the following terms: response to virus, defense response to virus, defense response to symbiont, negative regulation of viral genome replication, regulation of viral genome replication, negative regulation of viral process, viral life cycle and cytosolic pattern recognition receptor signaling pathway, etc. In the KEGG (Fig. 7B) pathway enrichment analysis, overlapping genes were mainly related to the following pathways. Viral protein interaction with cytokine and cytokine receptor, Influenza A, Coronavirus disease – COVID – 19, Inflammatory bowel disease, Cytokine – cytokine receptor interaction, RIG – I–like receptor signaling pathway, Rheumatoid arthritis and Such as IL – 17 signaling pathway, etc. The results suggest that OA and AS common core genes are associated with inflammatory and immune responses, which may be highly relevant to their pathogenesis.

Construction of a multi-factor regulatory network

Based on the prediction of hub genes from the TRRUST database, five of the key Hub genes obtained eight TFs that could regulate the corresponding genes. Then, based on the prediction results, the regulatory network of TF-mRNA was constructed using Cytoscape software (Fig. 8A), which included 13 nodes, and 20 edges. Next, we constructed a ceRNA network based on the above five characterized genes using starBase and miRanda database. The network contained 206 nodes and 226 edges, including the 5 characterized genes, 76 miRNAs, and 125 lncRNAs. finally, we constructed the ceRNA regulatory

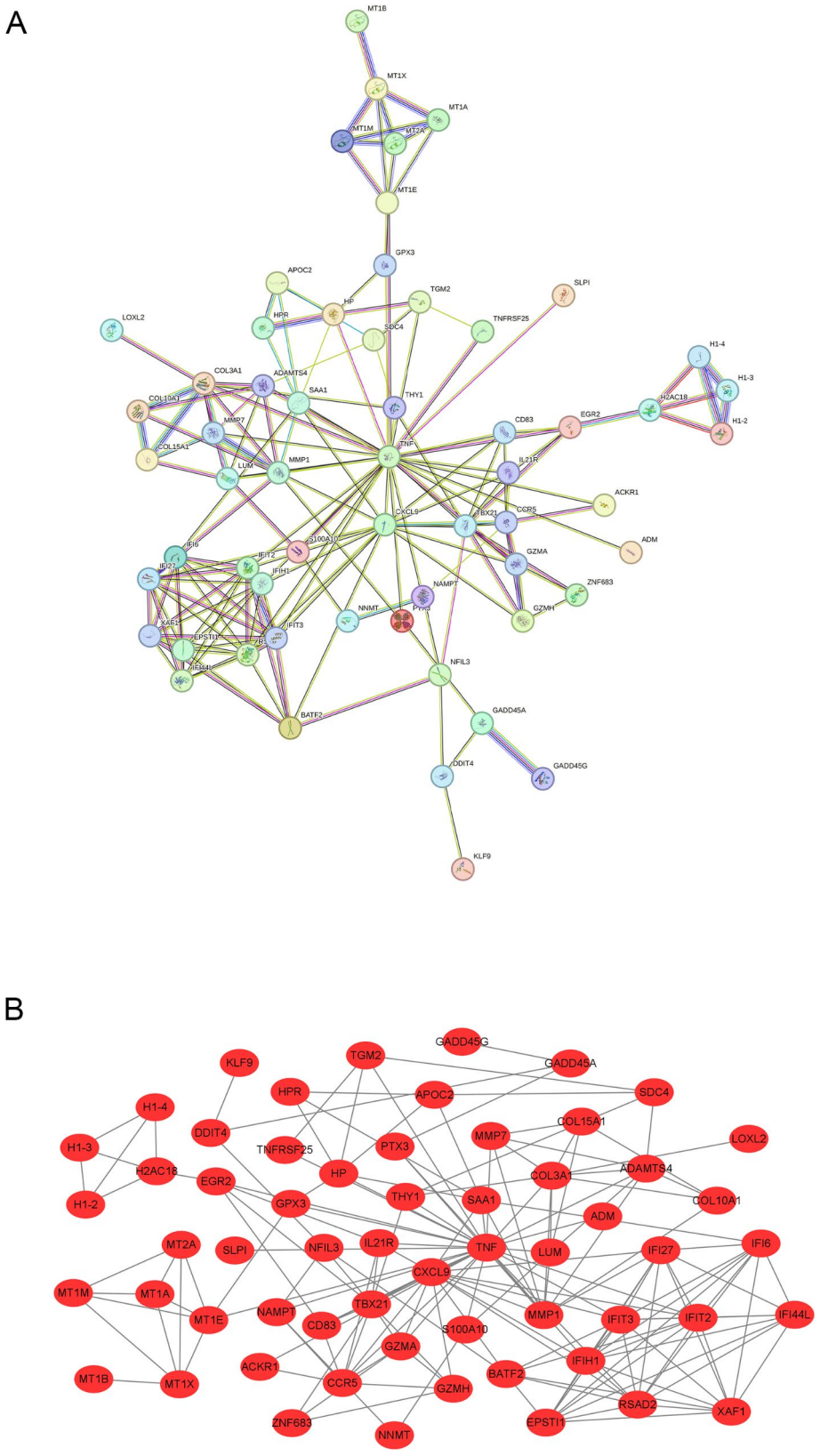

Fig. 3 PPI networks and identification of hub genes. **a**: PPI networks of common DEGs constructed in the STRING database. **b**: PPI networks of overlapping DEGs constructed by Cytoscape software

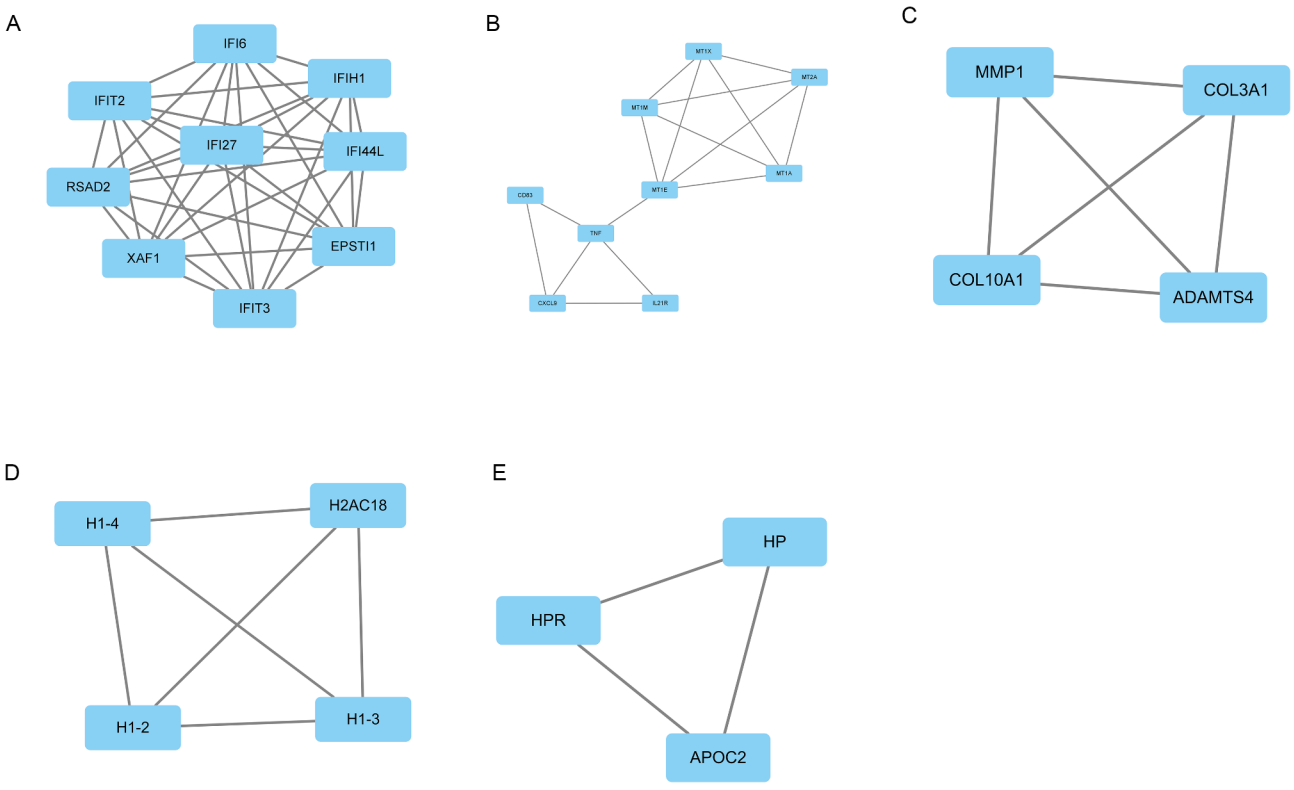

Fig. 4 Acquisition of sub-networks.A-E: Five gene clusters with high connectivity obtained by MCODE algorithm in PPI network

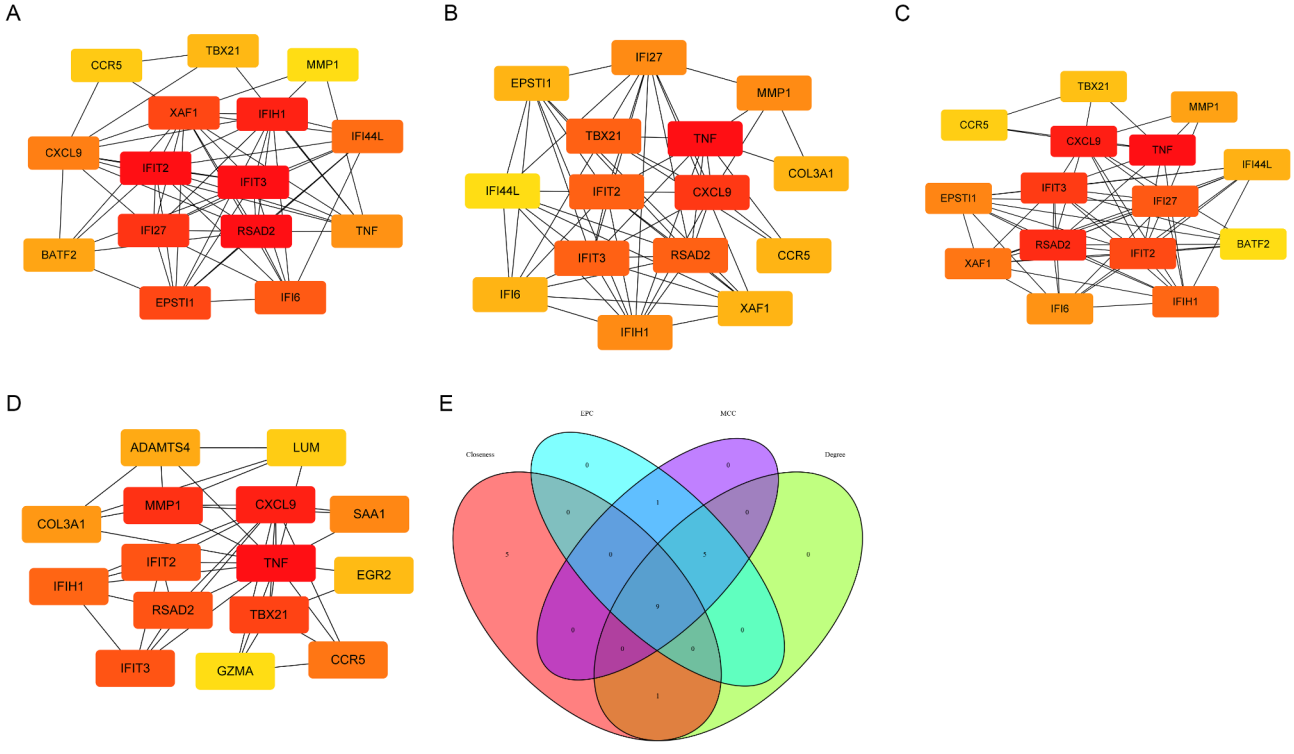

Fig. 5 Screening of key genes: 9 hub genes were identified by taking the intersection of the top 15 genes in four algorithms (MCC, Degree, EPC, and Closeness) of the cytoHubba plugin. Figure A-D: Schematic representation of the top 15 key genes selected by MCC, Degree, EPC, and Closeness, respectively. Figure E: Venn diagram showing the final key genes obtained from the intersection of the four algorithms

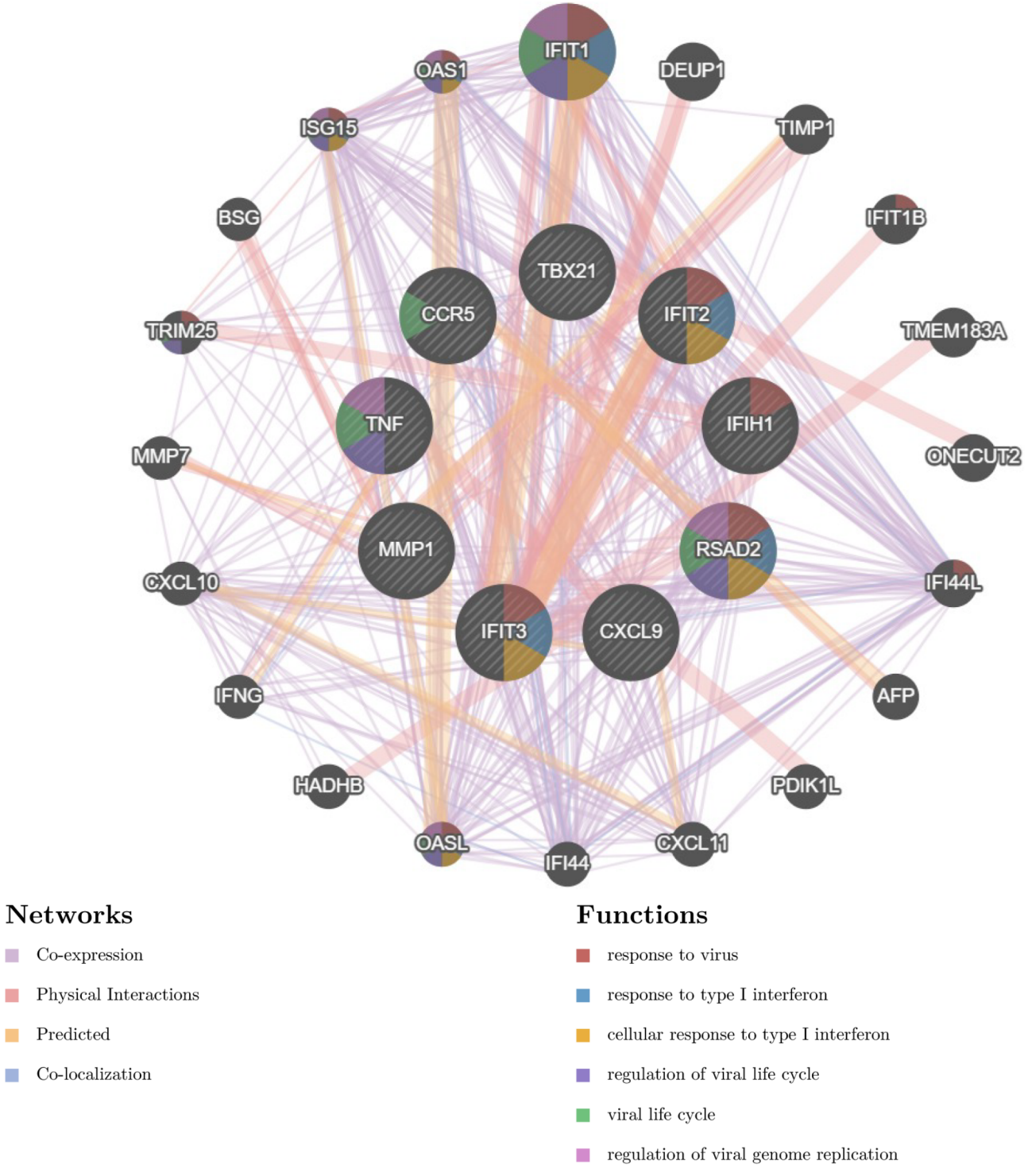

Fig. 6 Gene-gene interaction network of DEG analyzed using the GeneMANIA database. The figure shows the 20 most frequently altered neighboring genes. The predicted genes are located in the outer circle and the core genes are located in the inner circle DEG: Differentially Expressed Genes

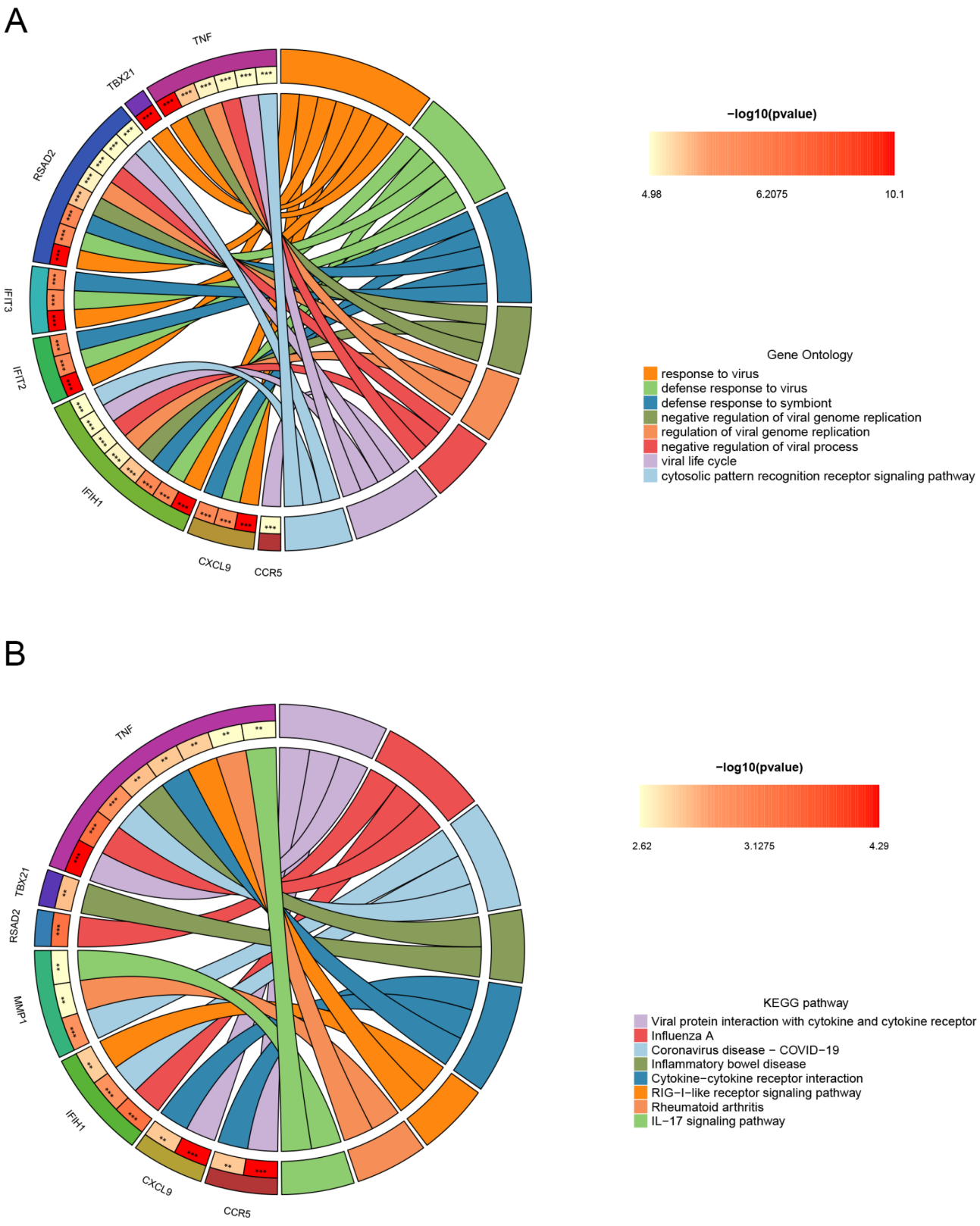

Fig. 7 Enrichment analysis of Hub genes. A and A are the results of GO and KEGG enrichment analysis of hub genes presented in the form of circle plots, respectively. The top eight most significantly enriched entries are shown in the circle plot. The outermost circle is the term on the right, and the inner circle on the left represents the significant P-value for the corresponding pathway of the gene

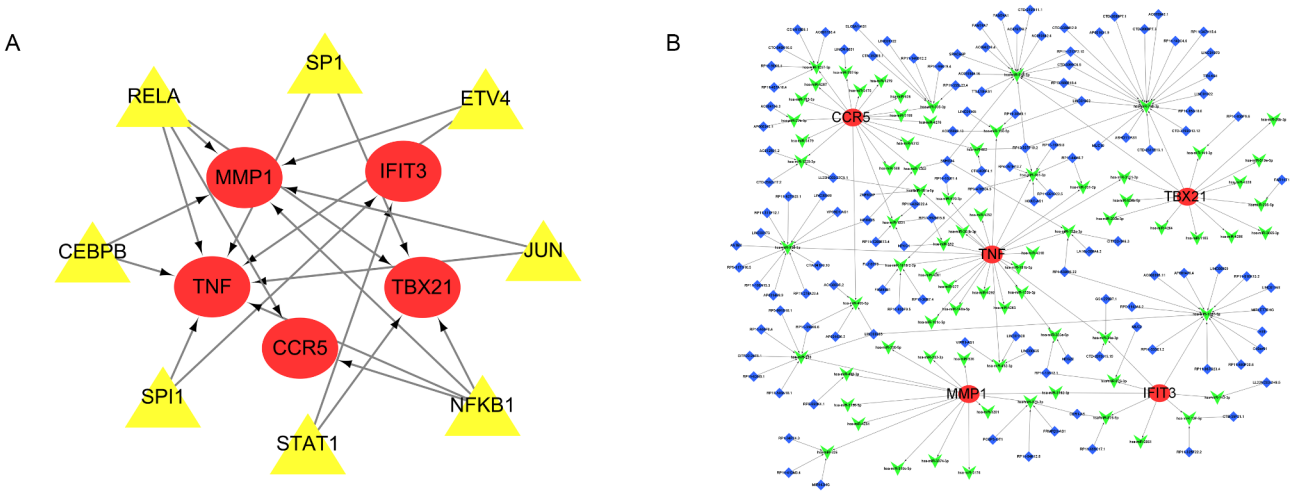

Fig. 8 Construction of multifactorial regulatory network.A: TF-miRNA regulatory network. Based on the TRRUST database, we constructed the TF-mRNA regulatory network of Hub genes using Cytoscape. Hub genes were labeled with red ovals; TF was labeled with yellow triangles. B: The ceRNA regulatory network of the above Hub genes. Based on the starBase and miRanda databases, we constructed the ceRNA regulatory network of the Hub genes for which TF was obtained using Cytoscape. Hub genes are labeled with red ovals; miRNAs are labeled with green inverted triangles; and lncRNAs are indicated by blue diamonds

network of Hub genes using Cytoscape software (e.g., Fig. 8B).

Screening for gene-targeted drugs

We collected small molecule drugs from the DSigDB database (https://dgidb.genome.wustl.edu/) collected small molecule drugs that regulate the expression of Hub genes, including three major classes of drugs: Approved, Antineoplastic and Immunotherapies. We identified a total of 96 drugs that regulate 3 Hub genes, 17 that regulate *MMP1*, 11 that regulate *CCR5*, and 68 that regulate *TNF* (see S1 file). From their results, 10 drugs each were selected for their mode of interaction with the genes and presented as network diagrams using Cytoscape software (Fig. 9).

Hub gene diagnostic performance analysis

We assessed the diagnostic effect of the 9 Hub genes by plotting ROC curves (Figs. 10 and 11). In the OA dataset, *CCR5* (AUC:0.785), *CXCL9* (AUC:0.845), *IFIH1* (AUC:0.823), *IFIT2* (AUC:0.925), *IFIT3* (AUC:0.870), *MMP1* (AUC:0.772), *RSAD2* (AUC:0.710), *TBX21* (AUC:0.773) and *TNF* (AUC:0.755) showed relatively good diagnostic efficiency in differentiating OA patients from healthy controls. In the AS dataset, *CCR5* (AUC:0.943), *CXCL9* (AUC:0.762), *IFIH1* (AUC:0.973), *IFIT2* (AUC:0.882), *IFIT3* (AUC:0.890), *MMP1* (AUC:0.867), *RSAD2* (AUC:0.844), *TBX21* (AUC:0.857) and *TNF* (AUC:0.958) showed better diagnostic performance in distinguishing AS from healthy individuals. Overall, the nine Hub genes we screened had strong diagnostic performance in both the OA dataset and the AS dataset.

Immune infiltration analysis

Using two previous enrichment analyses as well as GeneMANIA PPI analyses of the nine core genes and their 20 interacting genes, we found that the differential genes for both OA and AS diseases were immunologically related. Therefore, we calculated the content of each immune cell in the experimental versus control groups in both datasets using the ssGSEA algorithm. The results of the analysis (Fig. 12A and B) demonstrated significant changes in the immune landscape in OA and AS compared to the control group. In addition, correlation analysis showed that seven of the nine Hub key genes in OA were strongly correlated with immunity, with the exception of *MMP1* and *RSAD2* (Fig. 12C). In contrast, all of the nine Hub genes in AS were highly correlated with immunity (Fig. 12D). Taken together, different degrees of immune cell infiltration for different diseases may serve as potential therapeutic targets for the disease. In particular, *CCR5*, *CXCL9*, *TBX21*, and *TNF* are positively correlated with the majority of immune cells in both OA and AS, which may serve as a common potential immunotherapeutic target for concurrently suffering from both diseases.

Discussion

In an observational study, the authors found that osteoarthritis was a common complication in patients with cardiovascular disease [20.9% (19.5-23.5%)] [24]. Some investigations have shown that OA is associated with an increased risk of cardiovascular disease [25]. Although epidemiological studies has linked OA and AS, currently there are no reports on disease-wide exploration of underlining molecular mechanisms using computational

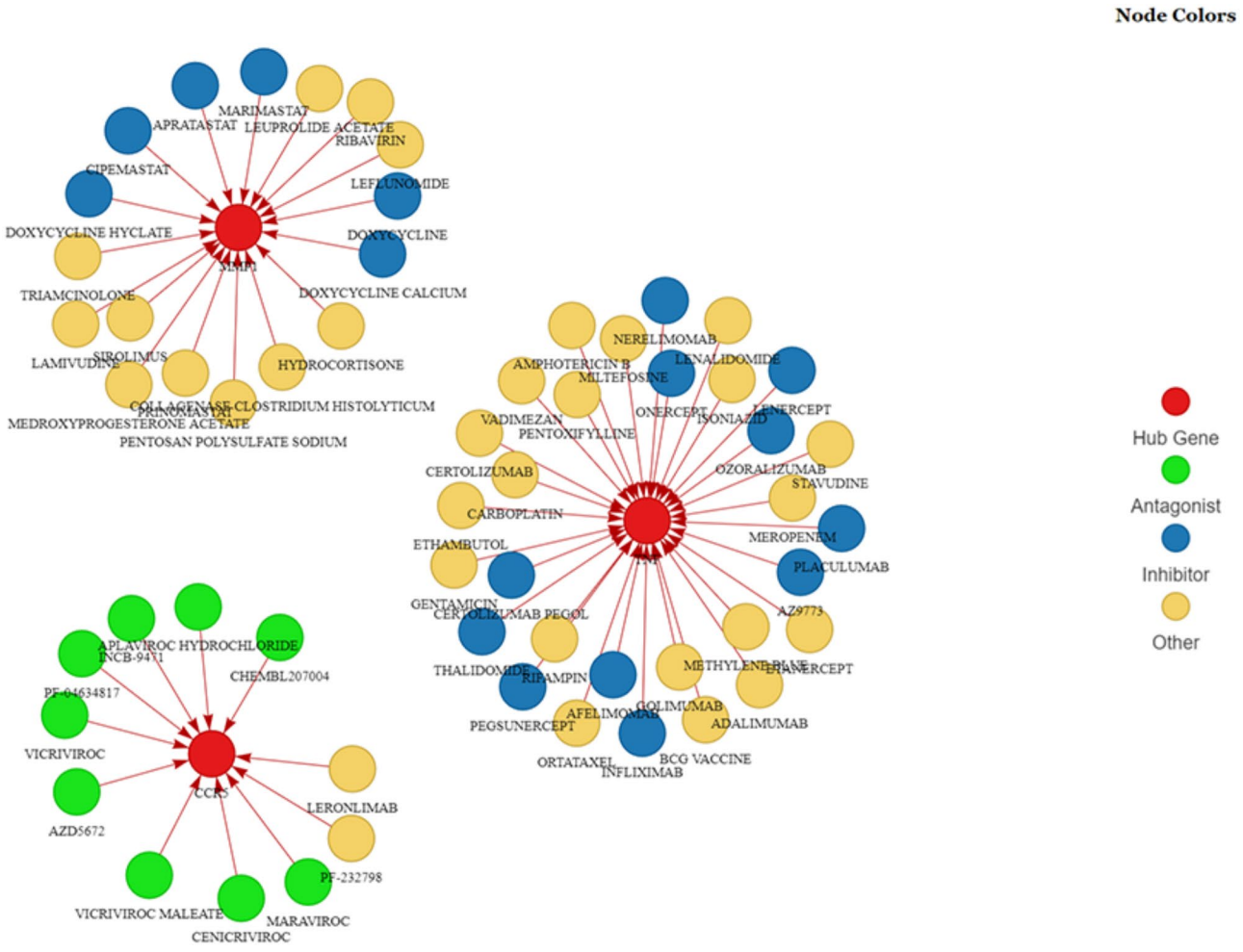

Fig. 9 Schematic representation of the top 10 drugs targeting Hub genes. The red circle represents genes, the green circle represents antagonist drugs, the blue circle represents inhibitor drugs, and the brown circle represents other drugs

analytic approaches. Therefore, we attempt to explore the common biological functions, pathways, and genetic features between OA and AS with bioinformatics methods, and further investigate the interrelationships between OA and AS. In this study, 91 common DEGs were identified. Enrichment analysis showed that these co-differentially expressed genes are significantly involved in the immune system and related immune signaling pathways. Subsequently, nine Hub genes (*CCR5*, *CXCL9*, *IFIH1*, *IFIT2*, *IFIT3*, *MMP1*, *RSAD2*, *TBX21*, and *TNF*) were identified in the PPI network according to four algorithms (Degree, MCC, Closeness, and EPC) in the Cytohubba plugin. Functional annotation analysis and co-expression network analysis of Hub genes re-emphasized the importance of the immune system in OA and AS. To verify the diagnostic value of the core genes, we assessed the diagnostic performance of the resulting core genes by plotting receiver operator characteristic (ROC) curves and observing the area under the curve (AUC). In addition, we predicted target gene drugs and constructed TF-mRNA as well as ceRNA regulatory networks to further elucidate the potential biological roles of the core genes and how they are regulated. These regulatory methods and the prediction of related drugs are beneficial for further exploring the common pathogenesis of OA and AS, providing new directions for laboratory research and clinical drug development in the future. Finally, the immune infiltration of OA and AS was analyzed and compared based on the ssGSEA algorithm, and the correlation between Hub genes and infiltrating immune cells was evaluated to reveal the related immune mechanisms. We conducted two tasks in the immunological analysis section. Firstly, we separately explored the immune differences between OA and AS and healthy control groups, indicating that the immune system plays a crucial role in the pathogenesis of OA and AS. Secondly, we analyzed the correlation between Hub genes and immune cells, indicating that Hub genes may affect the occurrence and development of diseases through the immune system. These results deepen our

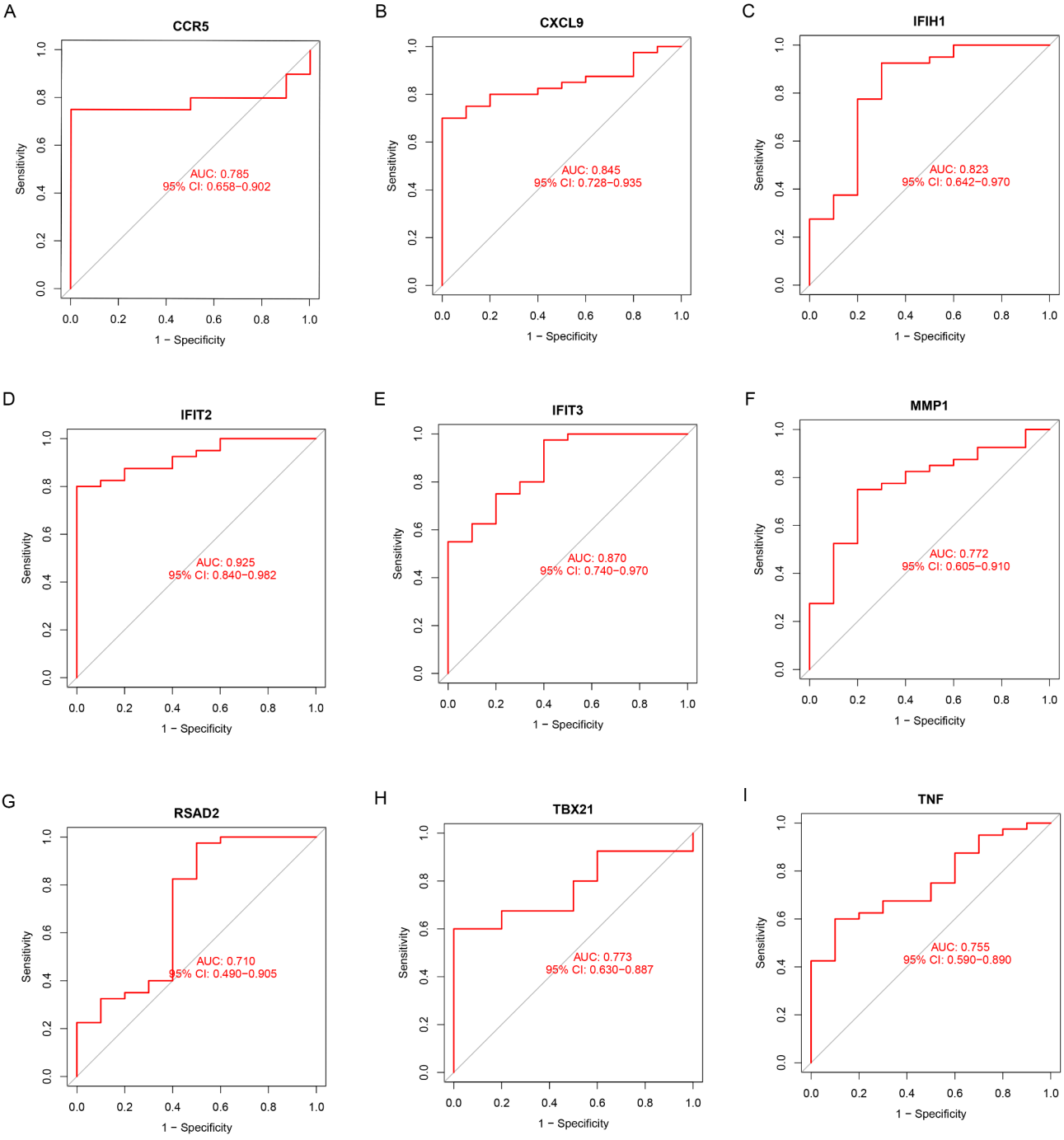

Fig. 10 ROC curves used in the GSE51588 dataset to assess the accuracy of the Hub gene logistic regression analysis. A-I were the Hub genes CCR5 (AUC:0.785), CXCL9 (AUC:0.845), IFIH1 (AUC:0.823), IFIT2 (AUC:0.925), IFIT3 (AUC:0.870), MMP1 (AUC:0.772), RSAD2 (AUC:0.710), respectively, TBX21 (AUC:0.773) and TNF (AUC:0.755) in the GSE51588 dataset were analyzed by ROC curves

understanding of the bone-vascular axis concept and may help to unravel the molecular mechanisms between OA and AS. To our knowledge, this is the first time that the hypothesis of OA and AS comorbidity has been studied by integrating data from various public databases. By conducting differential analysis and drawing receiver operating characteristic (ROC) curves and observing the area under the curve (AUC values all greater than 0.7), we preliminarily identified 9 central genes (*CCR5*, *CXCL9*, *IFIH1*, *IFIT2*, *IFIT3*, *MMP1*, *RSAD2*, *TBX21*, and *TNF*) that contribute to OA and AS.

CCR5, as a receptor for inflammatory chemokines, increases intracellular calcium levels and is widely expressed in T cells, smooth muscle endothelial cells,

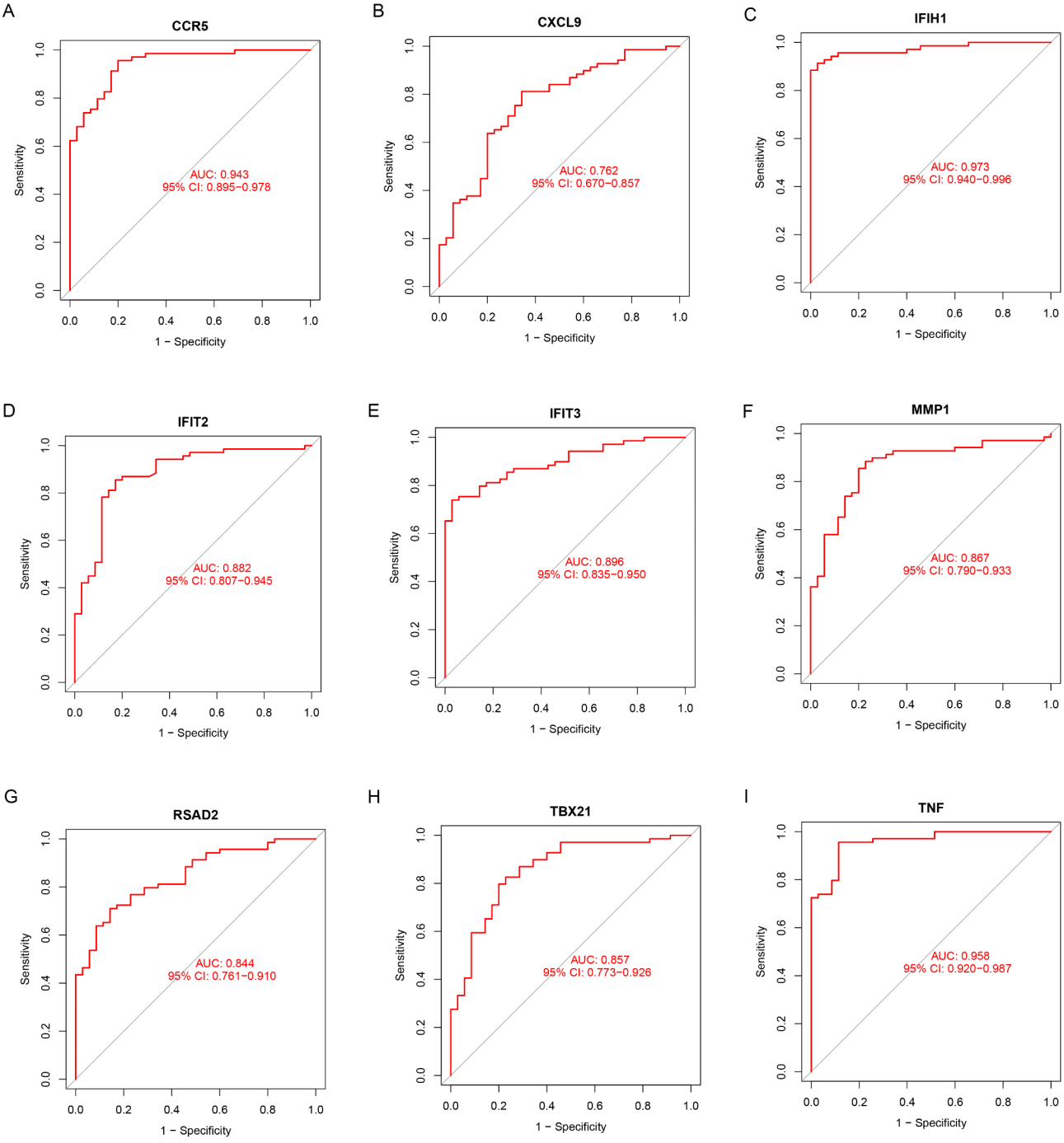

Fig. 11 ROC curves used in the GSE100927 dataset to assess the accuracy of the Hub gene logistic regression analysis. A-I were the Hub genes CCR5 (AUC:0.943), CXCL9 (AUC:0.762), IFIH1 (AUC:0.973), IFIT2 (AUC:0.882), IFIT3 (AUC:0.890), MMP1 (AUC:0.867), RSAD2 (AUC:0.844), respectively, TBX21 (AUC:0.857) and TNF (AUC:0.958) in the GSE100927 dataset were analyzed by ROC curves

epithelial cells and even parenchymal cells [26]. Studies have shown that *CCR5* expression is associated with HIV infection, cell proliferation, migration, angiogenesis, metastasis, and survival [27]. CCR5 has clear expression in periosteum as well as skeletal stem cells. It has been shown that treatment with CCL5 induces P-SSC migration and promotes fracture healing in vivo, and conversely *CCR5* deficiency, *CCR5* inhibition, or localized P-SSC ablation reduces osteoblast numbers and delays bone healing [28]. CCR5 transports blood monocytes to atherosclerotic plaques to promote the progression of AS [29]. It has been shown that treatment with a *CCR5* blocker as a model mouse resulted in a 70% reduction in plaque volume and a 50% reduction in monocyte/

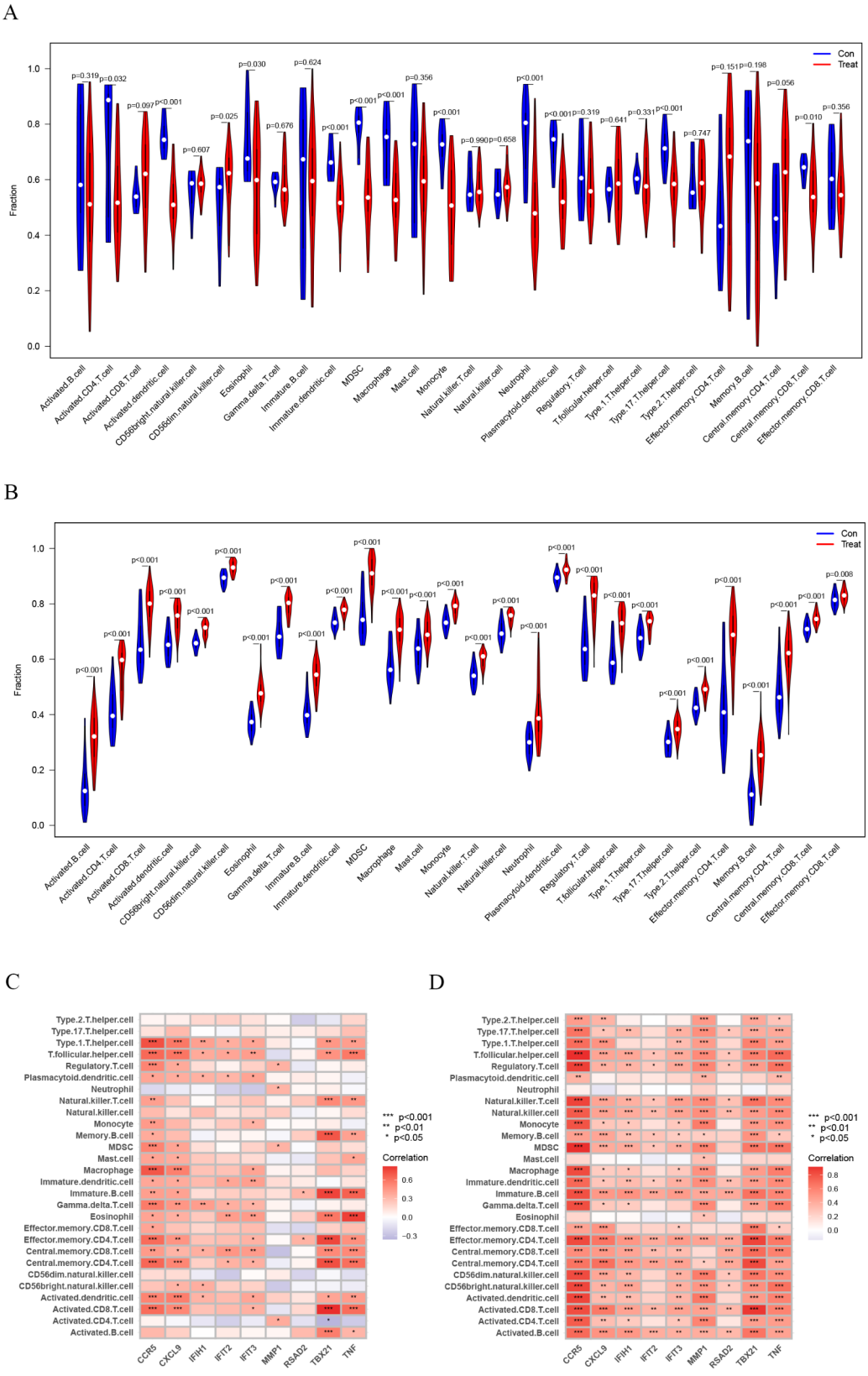

Fig. 12 Results of ssGSEA immune infiltration analysis. **A**: Box line plot of the expression of 28 immune cells between OA and controls in the GSE51588 dataset. **B**: Box line plot of 28 immune cell expressions between AS and controls in the GSE100927 dataset. **C**: Correlation between Hub gene expression and immune cell infiltration in GSE51588. **D**: Correlation between Hub gene expression and immune cell infiltration in GSE100927. Red squares indicate positive correlations and blue squares indicate negative correlations; darker squares indicate stronger correlations

macrophage infiltration [30]. T cells in the vessel wall of AS express high levels of CCR5 [31]. We hypothesized that CCR5 may contribute to disease progression by participating in the chemotaxis process of OA and AS inflammatory cells. CXCL9 is a small cytokine belonging to the CXC heme family, which has been shown to be associated with hypertension, diabetes, obesity and lung cancer [32–35]. All of these diseases are closely related to OA and AS. A bioinformatics study has shown that *IFIH1*, *IFIT2*, and *IFIT3* are differentially expressed in AS, which has been validated in carotid artery tissues from AS patients using qRT-PCR assay [36]. This study also showed that memory B cells and resting dendritic cells were positively correlated with the expression of *IFIH1*, *IFIT2* and *IFIT3*, and neutrophils were positively correlated with the expression of *IFIH1* [36]. This suggests that these genes may regulate the development of AS by modulating the immune microenvironment in humans. However, we found that their role in OA is less studied, emphasizing their importance in future research.

MMPs are extracellular matrix (ECM) degrading enzymes, which can be involved in inflammatory and immune responses [37]. MMP1, also known as mesenchymal collagenase and fibroblast collagenase, was the first MMPs to be identified and isolated from human fibroblasts. It is a fibrillogenic collagenase that hydrolyzes collagen proteins (e.g., I, II, III, VII, VIII). MMP1 is abundantly expressed in cartilage from patients with osteoarthritis and acts on newly synthesized type II collagen. When chondrocytes are stimulated by unfavorable factors such as compression or injury, chondrocytes synthesize large amounts of MMP1 to break down the cartilage matrix. In addition, MMP1 directly degrades type II collagen, which results in the loss of attachment of proteoglycans to type II collagen. It indirectly leads to the loss of proteoglycans through the above effects, which further decreases the mechanical properties and deformability of cartilage, thus accelerating the degenerative process of articular cartilage [38]. The important role of MMP1 in the development of atherosclerotic lesions and the immune system has been experimentally demonstrated, and *MMP1* has been confirmed to be a potential target in atherosclerosis [39]. It has been shown that *RSAD2* expression can be inhibited by PRMT5 and thus inhibit osteoclast differentiation [40]. However, its specific mechanism of action in OA and AS is not clear and needs to be further investigated. The *TBX21* gene is often expressed in T cells. *TBX21* gene expression promotes T1 cell differentiation and also induces T1 cells to secrete - γ, as well as participating in T cell-mediated immune responses [41]. Studies have shown that progesterone can be used to prevent and treat bone-related diseases in women [42]. Studies have shown that estrogen can be used to treat patients with osteoporosis by decreasing the expression of *TBX21.*

It is well known that both OA and AS are very closely related to estrogen, which is very revealing for drug development. It is well known that tumor necrosis factor (TNF) is a cytokine that was identified early on to promote the development of inflammation, and it has received widespread attention as a master regulator of inflammation. TNF can activate the inflammatory response by activating the typical NF-κB pathway and the mitogen-activated protein kinase (MAPK) signaling pathway [43–45], and can also induce apoptosis or cell necrosis through the kinase receptor-interacting serine/threonine protein kinase 1 (RIPK1) pathway [44, 46, 47]. Therefore, the study of TNF is a promising strategy to alleviate inflammation. Currently, several biologics have been approved by the FAD for the inhibition of TNF to promote inflammation reduction in diseases such as rheumatoid arthritis (RA), ankylosing spondylitis (AS), juvenile idiopathic arthritis, and psoriatic arthritis [48, 49]. Most of these commonly used drugs are monoclonal antibodies (e.g., infliximab, adalimumab, trastuzumab, golizumab), which exhibit a high affinity for TNF, leading to competitive blockade of TNF-TNFR interactions leading to effective therapy [50, 51]. We found that TNF inhibitors have now been shown to alleviate the inflammatory response in osteoarthritis and myocardial infarction [52]. Nonetheless, the widespread use of TNF inhibitors is subject to many limitations, such as the disadvantages of significant side effects, high cost, and the need for long-term administration [46, 48, 49, 53]. Therefore, the study of *TNF* is still very important for the treatment of OA combined with AS.

The focus of this paper is to explore common hub genes and immune infiltration profiles in OA and AS. Although the results are very satisfactory, there are some limitations of our study: firstly, this paper is a retrospective study and external experiments are still needed to further validate our conclusions. Second, drug-gene interaction pairs and TF-mRNA and ceRNA regulatory networks could provide clues for further exploration of core genes, but the exact roles still need to be revealed by more experiments. Third, the functions of hub genes and immune cells need to be validated and further explored in vitro and in vivo.

Conclusion

In summary, the present study preliminarily explored the differentially expressed genes in OA and AS and the potential common molecular mechanisms underlying the risk of developing OA and AS by bioinformatics methods. Nine hub genes (*CCR5*, *CXCL9*, *IFIH1*, *IFIT2*, *IFIT3*, *MMP1*, *RSAD2*, *TBX21* and *TNF*) were identified by PPI network construction. This study provides new insights

into the molecular mechanisms of osteoarthritis complicating atherosclerosis as well as diagnostic and therapeutic ideas.

Supplementary Information

The online version contains supplementary material available at https://doi.org/10.1186/s12891-025-08563-6.

Supplementary Material 1
Supplementary Material 2
Supplementary Material 3
Supplementary Material 4
Supplementary Material 5
Supplementary Material 6
Supplementary Material 7
Supplementary Material 8
Supplementary Material 9
Supplementary Material 10
Supplementary Material 11
Supplementary Material 12
Supplementary Material 13
Supplementary Material 14

Author contributions

Hua Zhang: Put forward the topic, and give the idea, and finally review. Yingchao Jin: Collecting data, organizing data, writing manuscripts.

Funding

Hebei Provincial Natural Science Foundation(H2021206391).

Data availability

No datasets were generated or analysed during the current study.

Declarations

Ethics approval and consent to participate.

Not applicable.

Consent for publication

Not applicable.

Competing interests

The authors declare no competing interests.

Received: 15 November 2023 / Accepted: 20 March 2025
Published online: 07 May 2025

References

1. Barbour KE, et al. Vital signs: prevalence of Doctor-Diagnosed arthritis and arthritis-Attributable activity Limitation - United States, 2013–2015. MMWR Morb Mortal Wkly Rep. 2017;66(9):246–53.
2. Loeser RF, et al. Osteoarthritis: a disease of the joint as an organ. Arthritis Rheum. 2012;64(6):1697–707.
3. Sagar DR, et al. Osteoprotegerin reduces the development of pain behaviour and joint pathology in a model of osteoarthritis. Ann Rheum Dis. 2014;73(8):1558–65.
4. Glyn-Jones S, et al. Osteoarthr Lancet. 2015;386(9991):376–87.
5. Global, regional, and national incidence, prevalence, and years lived with disability for 310 diseases and injuries, 1990–2015: a systematic analysis for the Global Burden of Disease Study 2015. Lancet. 2016;388(10053):1545–602.
6. Hunter DJ, Bierma-Zeinstra S. Osteoarthr Lancet. 2019;393(10182):1745–59.
7. Puig-Junoy J, Ruiz A, Zamora. Socio-economic costs of osteoarthritis: a systematic review of cost-of-illness studies. Semin Arthritis Rheum. 2015;44(5):531–41.
8. Zhang Z, Salisbury D, Sallam T. Long noncoding RNAs in atherosclerosis: JACC review topic of the week. J Am Coll Cardiol. 2018;72(19):2380–90.
9. Schaftenaar F, et al. Atherosclerosis: the interplay between lipids and immune cells. Curr Opin Lipidol. 2016;27(3):209–15.
10. Hussain SM, et al. Vascular pathology and osteoarthritis: A systematic review. J Rheumatol. 2020;47(5):748–60.
11. Findlay DM. Vascular pathology and osteoarthritis. Rheumatology (Oxford). 2007;46(12):1763–8.
12. Zelzer E, et al. Skeletal defects in VEGF(120/120) mice reveal multiple roles for VEGF in skeletogenesis. Development. 2002;129(8):1893–904.
13. Maes C, et al. Osteoblast precursors, but not mature osteoblasts, move into developing and fractured bones along with invading blood vessels. Dev Cell. 2010;19(2):329–44.
14. Shao JS, Cai J, Towler DA. Molecular mechanisms of vascular calcification: lessons learned from the aorta. Arterioscler Thromb Vasc Biol. 2006;26(7):1423–30.
15. Thompson B, Towler DA. Arterial calcification and bone physiology: role of the bone-vascular axis. Nat Rev Endocrinol. 2012;8(9):529–43.
16. Cui Z, et al. Halofuginone attenuates osteoarthritis by Inhibition of TGF-β activity and H-type vessel formation in subchondral bone. Ann Rheum Dis. 2016;75(9):1714–21.
17. Romeo SG, et al. Endothelial proteolytic activity and interaction with non-resorbing osteoclasts mediate bone elongation. Nat Cell Biol. 2019;21(4):430–41.
18. Zhu S, et al. Subchondral bone osteoclasts induce sensory innervation and osteoarthritis pain. J Clin Invest. 2019;129(3):1076–93.
19. MacDonald IJ et al. Implications of angiogenesis involvement in arthritis. Int J Mol Sci, 2018. 19(7).
20. Yao M, et al. Exploration of the shared gene signatures and molecular mechanisms between systemic lupus erythematosus and pulmonary arterial hypertension: evidence from transcriptome data. Front Immunol. 2021;12:658341.
21. Chin CH, et al. CytoHubba: identifying hub objects and sub-networks from complex interactome. BMC Syst Biol. 2014;8(Suppl 4):S11.
22. Finotello F, Trajanoski Z. Quantifying tumor-infiltrating immune cells from transcriptomics data. Cancer Immunol Immunother. 2018;67(7):1031–40.
23. Bindea G, et al. Spatiotemporal dynamics of intratumoral immune cells reveal the immune landscape in human cancer. Immunity. 2013;39(4):782–95.
24. Tran J, et al. Patterns and Temporal trends of comorbidity among adult patients with incident cardiovascular disease in the UK between 2000 and 2014: A population-based cohort study. PLoS Med. 2018;15(3):e1002513.
25. Nielen MM, et al. Cardiovascular disease prevalence in patients with inflammatory arthritis, diabetes mellitus and osteoarthritis: a cross-sectional study in primary care. BMC Musculoskelet Disord. 2012;13:150.
26. Velasco-Velázquez M, Xolalpa W, Pestell RG. The potential to target CCL5/CCR5 in breast cancer. Expert Opin Ther Targets. 2014;18(11):1265–75.
27. Zeng Z, et al. CCL5/CCR5 axis in human diseases and related treatments. Genes Dis. 2022;9(1):12–27.
28. Ortinau LC, et al. Identification of functionally distinct Mx1 + αSMA + Periosteal skeletal stem cells. Cell Stem Cell. 2019;25(6):784–e7965.
29. Tacke F, et al. Monocyte subsets differentially employ CCR2, CCR5, and CX3CR1 to accumulate within atherosclerotic plaques. J Clin Invest. 2007;117(1):185–94.
30. Cipriani S, et al. Efficacy of the CCR5 antagonist Maraviroc in reducing early, ritonavir-induced atherogenesis and advanced plaque progression in mice. Circulation. 2013;127(21):2114–24.
31. Joy MT, et al. CCR5 is a therapeutic target for recovery after stroke and traumatic brain injury. Cell. 2019;176(5):1143–e115713.
32. Mikolajczyk TP, et al. Role of inflammatory chemokines in hypertension. Pharmacol Ther. 2021;223:107799.
33. Wang Y, et al. Analysis of key genes and their functions in placental tissue of patients with gestational diabetes mellitus. Reprod Biol Endocrinol. 2019;17(1):104.
34. Harakeh S, et al. Chemokines and their association with body mass index among healthy Saudis. Saudi J Biol Sci. 2020;27(1):6–11.

35. Ding Q, et al. CXCL9: evidence and contradictions for its role in tumor progression. Cancer Med. 2016;5(11):3246–59.
36. Dong R, et al. Identification of immune-related biomarkers and construction of regulatory network in patients with atherosclerosis. BMC Med Genomics. 2022;15(1):245.
37. Ainiala H, et al. Increased serum matrix metalloproteinase 9 levels in systemic lupus erythematosus patients with neuropsychiatric manifestations and brain magnetic resonance imaging abnormalities. Arthritis Rheum. 2004;50(3):858–65.
38. Homandberg GA. Potential regulation of cartilage metabolism in osteoarthritis by fibronectin fragments. Front Biosci. 1999;4:D713–30.
39. Fletcher EK, et al. Deficiency of MMP1a (Matrix metalloprotease 1a) collagenase suppresses development of atherosclerosis in mice: translational implications for human coronary artery disease. Arterioscler Thromb Vasc Biol. 2021;41(5):e265–79.
40. Dong Y, et al. Inhibition of PRMT5 suppresses osteoclast differentiation and partially protects against ovariectomy-induced bone loss through down-regulation of CXCL10 and RSAD2. Cell Signal. 2017;34:55–65.
41. Lai N, et al. Regulatory effect of Catalpol on Th1/Th2 cells in mice with bone loss induced by Estrogen deficiency. Am J Reprod Immunol. 2015;74(6):487–98.
42. Prior JC. Progesterone for the prevention and treatment of osteoporosis in women. Climacteric. 2018;21(4):366–74.
43. Liu T, et al. NF-κB signaling in inflammation. Signal Transduct Target Ther. 2017;2:17023.
44. Annibaldi A, Meier P. Checkpoints in TNF-Induced cell death: implications in inflammation and cancer. Trends Mol Med. 2018;24(1):49–65.
45. Croft M, Siegel RM. Beyond TNF: TNF superfamily cytokines as targets for the treatment of rheumatic diseases. Nat Rev Rheumatol. 2017;13(4):217–33.
46. Kalliolias GD, Ivashkiv LB. TNF biology, pathogenic mechanisms and emerging therapeutic strategies. Nat Rev Rheumatol. 2016;12(1):49–62.
47. Blaser H, et al. TNF and ROS crosstalk in inflammation. Trends Cell Biol. 2016;26(4):249–61.
48. Savvides SN, Elewaut D. Small-molecule inhibitors get pro-inflammatory TNF into shape. Nat Rev Rheumatol. 2020;16(4):189–90.
49. Salomon BL. Insights into the biology and therapeutic implications of TNF and regulatory T cells. Nat Rev Rheumatol. 2021;17(8):487–504.
50. Song MY, et al. Characterization of a novel anti-human TNF-alpha murine monoclonal antibody with high binding affinity and neutralizing activity. Exp Mol Med. 2008;40(1):35–42.
51. Steeland S, Libert C, Vandenbroucke RE. A new venue of TNF targeting. Int J Mol Sci, 2018. 19(5).
52. Zheng W, et al. Simplified α(2)-macroglobulin as a TNF-α inhibitor for inflammation alleviation in osteoarthritis and myocardial infarction therapy. Biomaterials. 2023;301:122247.
53. Chen AY, Wolchok JD, Bass AR. TNF in the era of immune checkpoint inhibitors: friend or foe? Nat Rev Rheumatol. 2021;17(4):213–23.

Publisher's note

Springer Nature remains neutral with regard to jurisdictional claims in published maps and institutional affiliations.